Relativistic nuclear structure effects in quasielastic neutrino scattering

Hungchong Kim,[1,*] J. Piekarewicz,[2,†] and C. J. Horowitz[1,‡]
[1]*Nuclear Theory Center and Department of Physics, Indiana University, Bloomington, Indiana 47408*
[2]*Supercomputer Computations Research Institute, Florida State University, Tallahassee, Florida 32306*
(Received 12 December 1994)

Charged-current cross sections are calculated for quasielastic neutrino and antineutrino scattering using a relativistic meson-nucleon model. We examine how nuclear-structure effects, such as relativistic random-phase-approximation (RPA) corrections and momentum-dependent nucleon self-energies, influence the extraction of the axial form factor of the nucleon. RPA corrections are important only at low-momentum transfers. In contrast, the momentum dependence of the relativistic self-energies changes appreciably the value of the axial-mass parameter M_A extracted from dipole fits to the axial form factor. Using Brookhaven's experimental neutrino spectrum we estimate the sensitivity of M_A to various relativistic nuclear-structure effects.

PACS number(s): 14.20.Dh, 13.15.+g, 21.60.Jz

I. INTRODUCTION

The strange-quark content of the nucleon has received considerable attention as a result of the measurement of the spin-dependent structure function of the proton by the European Muon Collaboration (EMC) [1]. Some analyses of the experiment suggest that a large portion of the spin of the proton is carried by strange quarks. One can attempt to resolve this "spin problem" by studying the strange-quark contribution to the vector (both electric and magnetic) and axial-vector form factors of the nucleon. Most likely, it will take a large number of measurements to determine all of these form factors separately. Moreover, there are important complications from radiative corrections [2], which hinder the extraction of strange-quark matrix elements from parity-violating electron scattering. Therefore, one anticipates a program of several electron experiments [3] which, combined with neutrino scattering data [4], will offer the most accurate strange-quark information.

Neutral-current neutrino scattering is sensitive to the strange-quark matrix elements of the nucleon — especially to the isoscalar component [5]. Complications arise, however, from the fact that most neutrino experiments measure a combination of elastic scattering from free protons plus quasielastic scattering from nucleons bound in nuclei. In the present work we examine how nuclear-structure corrections affect the extraction of strange-quark information.

The isoscalar part of the axial-vector form factor of the nucleon is characterized by the parameter g_A^s — the value of the isoscalar strange form factor at zero four-momentum transfer. Unfortunately, the extraction of g_A^s from the Brookhaven National Laboratory (BNL) experiment is complicated by low statistics [4]. Moreover, there is a strong correlation between the extracted value of g_A^s and the axial mass M_A obtained from dipole fits to the axial-vector form factor [6,7]. Indeed, the world-average value of M_A (1.032 ± 0.036 GeV) that the BNL group has used is significantly different from the one [1.09 ± 0.03 (stat)± 0.02 (syst) GeV] extracted later from a charged-current experiment [8]. Thus, this large difference in M_A is sufficient to change the value of g_A^s extracted from the BNL experiment and the conclusion of a nonzero strange-quark content from our previous neutral-current study [7]. Therefore determining the precise value of M_A is important for strangeness studies.

At relatively high-momentum transfer, the response of the nuclear target seems to be adequately described in a relativistic Fermi gas (RFG) model. Indeed, at a qualitative level, a RFG calculation of quasielastic (e, e') longitudinal and transverse responses agrees well with finite-nucleus results. However, is the RFG model accurate enough to determine the precise value of M_A? Currently, the BNL experiment claims an M_A value with an error of less than five percent. Is there any uncertainty comparable to this small error induced from nuclear-structure effects? It is the aim of this work to go beyond the RFG response and examine the sensitivity of quasielastic neutrino scattering, particularly M_A, to a variety of nuclear-structure corrections.

One such correction arises from long-range RPA correlations. In a recent paper, Singh and Oset used a nonrelativistic RPA formalism to study the nuclear response in quasielastic neutrino scattering [9]. They found RPA corrections to be large only at low-momentum transfers. Since most neutrino experiments [10] are carried out at medium- to high-momentum transfers, they concluded that the value of M_A extracted from these experiments is reliable.

In a relativistic description of the nuclear target, additional nuclear-structure corrections must be considered. According to quantum hadrodynamics (QHD) [11], the

*Electronic address: hung@iucf.indiana.edu
†Electronic address: jorgep@ds16.scri.fsu.edu
‡Electronic address: charlie@iucf.indiana.edu

saturation of nuclear matter arises from a cancellation of strong scalar (σ) and vector (ω) mean fields. The strong scalar field decreases the nucleon mass while the vector field shifts the four-momentum of the nucleon in the medium. These relativistic effects were not addressed in the nonrelativistic calculation and may provide interesting corrections to the RFG response.

In a charged-current reaction, the mean-field ground state can be characterized in terms of an effective nucleon mass that is reduced, relative to its free-space value, by the presence of the strong scalar field. In turn, the RPA response can be modeled from a $(\pi + \rho + g')$ residual isovector interaction. In a mean-field approximation, the effective nucleon mass is obtained from solving self-consistently the equations of motion at a given baryon density [11]. In the case of polarized electron scattering, the parity-violating asymmetry was found to be sensitive to the in-medium value of the nucleon mass [12]. This is an interesting result that should be incorporated in neutrino-scattering studies.

This paper is organized as follows. Section II presents the formalism for the cross section of inclusive neutrino scattering in a relativistic impulse approximation and in RPA. Results for the charged current cross section are presented in Sec. III, while Sec. IV is a summary.

II. FORMALISM

In a charged-current process, neutrinos (and antineutrinos) interact with nuclei via the exchange of charged weak-vector bosons ($W^{\pm}$) with the resulting production of charged leptons (electrons or muons) in the final state. In an inclusive process, where only the final leptons are detected, the most general expression for the cross section can be given in terms of a time-ordered product of current operators. From this general expression several approximations can be made depending on how one treats the ground state of the nucleus and its response to the external probe. In Sec. II A, we derive a general formalism for the inclusive process and discuss various approximations for the response in a mean-field approximation to the ground state. In Sec. II B we discuss the form of the nuclear current adopted in the calculation while Sec. II C contains a detailed description of the relativistic random phase approximation. Finally, in Sec. II D we discuss how the mean-field ground state is modified by the introduction of phenomenological momentum-dependent corrections to the nucleon self-energies.

A. General formalism

The scattering process we consider is shown in Fig. 1. An incoming neutrino with momentum k scatters off the nucleus via the exchange of weak-vector bosons producing a charged lepton with momentum k' in the final state. The initial and final states of the nucleus are denoted by $|\psi_i(p_i)\rangle$ and $|\psi_f(p_f)\rangle$, respectively. In Born approximation the inclusive cross section becomes proportional to

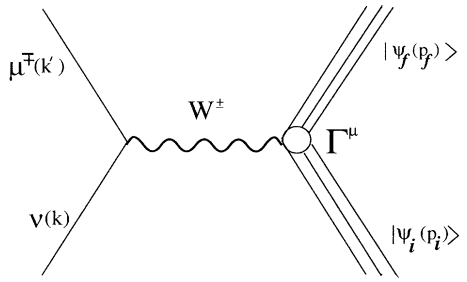

FIG. 1. Feynman diagram for charged-current neutrino scattering. The neutrino with momentum k scatters off a nucleus in a state $|\psi_i(p_i)\rangle$ and produces a muon or an electron with momentum k'.

the contraction of a leptonic and a hadronic tensor:

$$d\sigma \propto L_{\mu\nu} W^{\mu\nu} , \tag{1}$$

where the corresponding leptonic ($L_{\mu\nu}$) and hadronic ($W^{\mu\nu}$) tensors are given by

$$L_{\mu\nu} = 8[k'_\mu k_\nu - k \cdot k' g_{\mu\nu} + k'_\nu k_\mu \mp i\epsilon^{\alpha\mu\beta\nu} k'^{\alpha} k^{\beta}] , \tag{2}$$

$$W^{\mu\nu} = \sum_f (2\pi)^4 \, \delta^{(4)}(p_i + q - p_f) \, \langle \psi_i | \hat{J}^\mu(0) | \psi_f \rangle \times \langle \psi_f | \hat{J}^\nu(0) | \psi_i \rangle . \tag{3}$$

Here $\hat{J}^\mu$ is the weak charge-changing current operator of the nucleus, $q = k - k'$ is the momentum transfer to the nucleus, and the plus (minus) sign in $L_{\mu\nu}$ corresponds to antineutrino (neutrino) scattering. Note that our convention for the antisymmetric tensor is $\epsilon^{0123} \equiv 1$.

Now we introduce the current-current correlation function, or polarization tensor, as a time-ordered product of nuclear currents [13]

$$i\Pi^{\mu\nu}(q) = \int d^4x \, e^{iq\cdot x} \, \langle \psi_i | T(\hat{J}^\mu(x) \, \hat{J}^\nu(0)) | \psi_i \rangle . \tag{4}$$

The hadronic tensor, and therefore the cross section, can be directly related to the polarization tensor. In particular, it is easy to show that the cross section takes the following form

$$d\sigma \propto \mathrm{Im}\,(L_{\mu\nu} \Pi^{\mu\nu}) . \tag{5}$$

This expression is convenient for the evaluation of the inclusive response of a many-body system like the nucleus. In particular, various approximations can be made depending on how one calculates the ground state of the nucleus and its linear response to the external probe [14,15].

For the many-body current operator $\hat{J}_\mu$ we assume a simple one-body form:

$$\hat{J}_\mu(x) = \bar{\psi}(x) \Gamma_\mu \psi(x), \tag{6}$$

where $\psi(x)$ is a nucleon-field operator and Γ_μ is the weak-interaction vertex to be discussed below [see Eq. (13)]. Meson-exchange currents represent corrections to this one-body form and will be ignored throughout this pa-

per. In a mean-field approximation to the nuclear ground state the time-ordered product of currents can be evaluated readily using Wick's theorem, i.e.,

$$i\Pi^{\mu\nu} = \int \frac{d^4p}{(2\pi)^4} \mathrm{Tr}[G(p+q)\,\Gamma^\mu\,G(p)\,\Gamma^\nu]\,, \tag{7}$$

where $G(p)$ is the nucleon propagator that will be evaluated in various approximations.

The simplest approximation that we employ treats the nuclear ground state as a relativistic free Fermi gas. Here the nuclear response consists of the excitation of particle-hole pairs subject to the constraints imposed by energy-momentum conservation and the Pauli principle. The nucleon propagator differs from the well-known Feynman propagator only because of a finite-density correction arising from the filled Fermi sea [11],

$$G^o(p) = (\not{p} + M)\left[\frac{1}{p^2 - M^2 + i\epsilon} + \frac{i\pi}{E_{\mathbf{p}}}\delta(p_0 - E_{\mathbf{p}}) \times\theta(k_F - |\mathbf{p}|)\right]. \tag{8}$$

Note that we have introduced the Fermi momentum k_F and the free (on-shell) energy $E_{\mathbf{p}} = \sqrt{\mathbf{p}^2 + M^2}$. We call this approximation "impulse with M" in order to distinguish it from the self-consistent impulse approximation with an effective mass M^* that we now address.

One can improve the free Fermi-gas description by taking into account, at least at the mean-field level, the interaction between the nucleons in the nucleus. In a mean-field-theory approximation (MFT) to the Walecka model the propagation of a nucleon through the medium is modified by the presence of constant scalar and vector mean-fields. These potentials induce a shift in the mass and in the energy of a particle in the medium and give rise to a self-consistent nucleon propagator [11]:

$$G^*(p) = (\not{p}^* + M^*)\left[\frac{1}{p^{*2} - M^{*2} + i\epsilon} + \frac{i\pi}{E^*_{\mathbf{p}}}\delta(p^*_0 - E^*_{\mathbf{p}})\theta(k_F - |\mathbf{p}|)\right], \tag{9}$$

where the effective mass and energy are shifted from their free-space value by the scalar (S) and timelike component (V^0) of the mean fields,

$$M^* = M + S\,,\quad E^*_{\mathbf{p}} = \sqrt{\mathbf{p}^2 + M^{*2}}\,,$$
$$p^{*\mu} = (p^0 - V^0, \mathbf{p})\,. \tag{10}$$

These changes in the nucleon propagator induce a corresponding change in the polarization tensor, which is now written

$$i\Pi^{\mu\nu}_{MF} = \int \frac{d^4p}{(2\pi)^4} \mathrm{Tr}[G^*(p+q)\,\Gamma^\mu\,G^*(p)\,\Gamma^\nu]\,. \tag{11}$$

Note, in computing the response we integrate over the four-momentum of the nucleons, and the contribution from the constant vector potential can be eliminated by a simple change of variables. [This will not happen once momentum-dependent corrections are incorporated into the mean fields (see Sec. II D).] Formally the mean-field response is identical to that of a relativistic Fermi gas of nucleons with an effective mass M^*. We refer to this calculation as "impulse with M^*."

B. Impulse approximation

We start this section by writing the inclusive cross section, per neutron, for the charge-changing process as

$$\frac{d^2\sigma}{d\Omega_{k'}dE_\mu} = -\frac{G_F^2\cos^2\theta_c\,|\mathbf{k}'|}{32\pi^3\rho E_\nu}\,\mathrm{Im}\,(L_{\mu\nu}\Pi^{\mu\nu})\,. \tag{12}$$

Here $\rho = k_F^3/3\pi^2$ is the neutron (or proton) density of the system, θ_c the Cabbibo angle ($\cos^2\theta_c = 0.95$), G_F is the Fermi constant, $\mathbf{k}'$ the three-momentum of the outgoing lepton, and E_ν the energy of the incoming neutrino (or antineutrino).

In the impulse approximation the interaction between the incoming neutrino and a target nucleon is assumed to be the same as in free space. Hence, we employ a charge-changing current operator with single-nucleon form factors parameterized from on-shell data. That is (suppressing isospin labels),

$$\Gamma^\mu(q) = F_1(Q^2)\gamma^\mu + iF_2(Q^2)\sigma^{\mu\nu}\frac{q_\nu}{2M} - G_A(Q^2)\gamma^\mu\gamma^5 + F_p(Q^2)q^\mu\gamma^5\,,\quad (Q^2 \equiv \mathbf{q}^2 - q_0^2)\,. \tag{13}$$

The form factors F_1, F_2, G_A and F_p are given in Appendix A. The pseudoscalar form factor F_p is constructed from PCAC, and its contribution is suppressed by the small lepton mass.

Since Γ^μ has been expressed in terms of vector, tensor, axial-vector, and pseudoscalar vertices, the inclusive cross section requires the evaluation of a large set of nuclear-response functions. These are conveniently separated in the following way (note that the subscripts indicate the vertices involved):

$$\Pi^{\mu\nu}_{vv} = -i\int \frac{d^4p}{(2\pi)^4} \mathrm{Tr}[G(p+q)\,\gamma^\mu\,G(p)\,\gamma^\nu]\,, \tag{14}$$

$$\Pi^{\mu\nu}_{tt} = -i\int \frac{d^4p}{(2\pi)^4} \mathrm{Tr}\left[G(p+q)\,\frac{i\sigma^{\mu\alpha}q_\alpha}{2M} \times G(p)\,\frac{-i\sigma^{\nu\beta}q_\beta}{2M}\right], \tag{15}$$

$$\Pi^{\mu\nu}_{vt} = -i\int \frac{d^4p}{(2\pi)^4} \mathrm{Tr}\left[G(p+q)\,\gamma^\mu\,G(p)\,\frac{-i\sigma^{\nu\beta}q_\beta}{2M}\right], \tag{16}$$

$$\Pi^{\mu\nu}_{va} = -i\int \frac{d^4p}{(2\pi)^4} \mathrm{Tr}[G(p+q)\,\gamma^\mu\,G(p)\,\gamma^\nu\gamma^5] = -i\epsilon^{\mu\nu\alpha 0}\,q_\alpha\Pi_{va}\,, \tag{17}$$

$$\Pi^{\mu\nu}_{aa} = -i\int \frac{d^4p}{(2\pi)^4} \mathrm{Tr}[G(p+q)\,\gamma^\mu\gamma^5\,G(p)\,\gamma^\nu\gamma^5] = \Pi^{\mu\nu}_{vv} + g^{\mu\nu}\Pi_A\,, \tag{18}$$

$$\Pi^{\mu\nu}_{ap} = -i \int \frac{d^4p}{(2\pi)^4} \mathrm{Tr}[G(p+q)\,\gamma^\mu\gamma^5\,G(p)\,(-q^\nu)\gamma^5] = q^\mu q^\nu \Pi_{ap} \ , \tag{19}$$

$$\Pi^{\mu\nu}_{pp} = -i \int \frac{d^4p}{(2\pi)^4} \mathrm{Tr}[G(p+q)\,q^\mu\gamma^5\,G(p)\,(-q^\nu)\gamma^5] = q^\mu q^\nu \Pi_{pp} \ . \tag{20}$$

The various components of the polarization tensor can be computed in the Fermi-gas limit or in the mean-field approximation by using either $G^o(p)$ [Eq. (8)] or $G^*(p)$ [Eq. (9)], respectively. The imaginary parts of all these polarizations have been calculated analytically following the Ref. [16] and are given in Appendix B.

The polarizations $\Pi^{\mu\nu}_{vv}$, $\Pi^{\mu\nu}_{tt}$, and $\Pi^{\mu\nu}_{vt}$ are only sensitive to the Lorentz-vector part of the weak current and, thus, satisfy current conservation, $q_\mu \Pi^{\mu\nu} = \Pi^{\mu\nu} q_\nu = 0$. The conservation of the vector current plus Lorentz covariance imply that only two components of each of these polarizations are independent. These have been chosen to be the longitudinal and transverse components which are defined, for example in the the case of $\Pi^{\mu\nu}_{vv}$, as

$$\Pi^L_{vv} \equiv \Pi^{00}_{vv} - \Pi^{11}_{vv} = -\frac{q^2}{\mathbf{q}^2}\Pi^{00}_{vv} \ , \tag{21}$$

$$\Pi^T_{vv} \equiv 2\Pi^{22}_{vv} = 2\Pi^{33}_{vv} \ . \tag{22}$$

Here we have assumed a coordinate system with the $\hat{x} = \hat{1}$ axis along the direction of the three-momentum transfer $\mathbf{q}$. Using Lorentz covariance one can isolate the additional responses that arise from the other components of the current and obtain the following invariant amplitude

$$L_{\mu\nu}\Pi^{\mu\nu} = L_L R_L + L_T R_T \pm L_{va} R_{VA} + L_A R_A + L_p R_P \ . \tag{23}$$

The nuclear-structure information is fully contained in the various response functions which have been defined in terms of the above polarization tensors:

$$R_L = (F_1^2 + G_A^2)\ \Pi^L_{vv} + 2F_1F_2\ \Pi^L_{vt} + F_2^2\ \Pi^L_{tt} \ , \tag{24}$$

$$R_T = \frac{1}{2}[(F_1^2 + G_A^2)\ \Pi^T_{vv} + 2F_1F_2\ \Pi^T_{vt} + F_2^2\ \Pi^T_{tt}] \ , \tag{25}$$

$$R_P = 2G_A\ F_p\ \Pi_{ap} + F_p^2\ \Pi_{pp} \ , \tag{26}$$

$$R_A = G_A^2 \Pi_A \ , \tag{27}$$

$$R_{VA} = \left(F_1 + F_2\frac{M^*}{M}\right)\ G_A\ |\mathbf{q}|\ \Pi_{va} \ . \tag{28}$$

These response functions are multiplied by appropriate kinematical factors that could, in principle, be used to separate the individual responses

$$L_L \equiv -\frac{q^2}{\mathbf{q}^2}L_{00} - \frac{4m_\mu^2\ q_0}{\mathbf{q}^2}\left(4E_\nu - q_0 + \frac{q_0\ m_\mu^2}{q^2}\right) \ , \tag{29}$$

$$L_A \equiv 8(q^2 - m_\mu^2) \ , \tag{30}$$

$$L_T \equiv -\frac{q^2}{\mathbf{q}^2}L_{00} - \frac{4m_\mu^2}{\mathbf{q}^2}(4E_\nu\ q^0 - q^2 + m_\mu^2) - L_A \ , \tag{31}$$

$$L_p \equiv 4m_\mu^2\ (m_\mu^2 - q^2) = -\frac{1}{2}m_\mu^2\ L_A \ , \tag{32}$$

$$L_{va} \equiv -16\frac{q^2\ (E_\nu + E_\mu) + q_0\ m_\mu^2}{|\mathbf{q}|} \ . \tag{33}$$

Finally, we note that the plus (minus) sign in Eq. (23) should be used for neutrino (antineutrino) scattering.

C. Relativistic random phase approximation

In the present section we improve the simple particle-hole description of the response by incorporating many-body RPA correlations. Many-body correlations can be included by considering the residual interaction between the particle and the hole. For the present charge-changing reaction only isovector correlations are important. Yet, there might still be important effects associated with the isoscalar mean fields (e.g., M^*). Indeed, in a recent calculation we have shown that the reduction of the effective nucleon mass in the medium results in a quenching of the effective $NN\pi$ coupling which, in turn, is responsible for suppressing the predicted enhancement of the spin-longitudinal to spin-transverse ratio, in accordance with experiment [17]. For the residual isovector interaction we employ a simple relativistic generalization of the conventional $\pi + \rho + g'$ interaction [9,18]. The phenomenological Landau-Migdal parameter g' has been included to simulate the effect of repulsive short-range correlations. The RPA correction, $\Delta\Pi^{\mu\nu}_{\mathrm{RPA}}$, to the polarization tensor, $\Pi^{\mu\nu}$ in Eq. (12), is shown diagrammatically in Fig. 2(a). The RPA corrections are calculated from the dressed propagator, $\mathbf{D_{RPA}}$. This includes an infinite sum of the lowest-order (uncorrelated) polarization as illustrated in Fig. 2(b). Note, for the mean-field ground state, the nucleon propagators in the lowest-order polarization already include the isoscalar dressing due to the mean fields [see Eq. (9)].

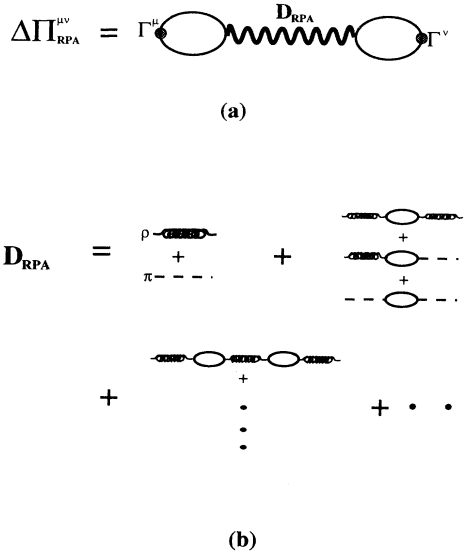

FIG. 2. A diagrammatic representation of the RPA correction $\mathbf{\Delta\Pi_{RPA}}$. The RPA propagator $\mathbf{D_{RPA}}$ is shown in (b).

The Lagrangian density describing the isovector component of the NN interaction is given by

$$\mathcal{L} = g_\rho \bar{\psi}\gamma^\mu \frac{\boldsymbol{\tau}}{2}\cdot\psi\boldsymbol{\rho}_\mu + f_\rho\bar{\psi}\sigma^{\mu\nu}\frac{\boldsymbol{\tau}}{2}\cdot\psi\frac{\partial_\mu}{2M}\boldsymbol{\rho}_\nu - \frac{f_\pi}{m_\pi}\bar{\psi}\gamma_5\gamma^\mu\boldsymbol{\tau}\psi\cdot\partial_\mu\boldsymbol{\pi} \ . \tag{34}$$

The ρ meson has a vector (g_ρ) as well as a tensor (f_ρ) coupling to the nucleon. The parameters of the model are obtained directly from the Bonn potential fit to NN properties and are given by $g_\rho^2/4\pi = 1.64$ and $f_\rho/g_\rho = 6.1$ [19] (note that our value for $g_\rho^2/4\pi$ is four times larger than the one quoted by the Bonn group simply because of our selection of $\boldsymbol{\tau}/2$, rather than $\boldsymbol{\tau}$, as the isospin vertex). With this form for the interaction Lagrangian the $NN\rho$ vertex becomes (combined with isospin matrices)

$$\Gamma_\mu^{NN\rho} = -\frac{i}{\sqrt{2}}\left(g_\rho\gamma_\mu + \frac{if_\rho\sigma_{\mu\nu}q^\nu}{2M}\right) , \tag{35}$$

while the ρ-meson propagator is given by

$$R_{\mu\nu}(q) = \frac{-g_{\mu\nu} + q_\mu q_\nu/m_\rho^2}{q^2 - m_\rho^2 + i\epsilon} \ . \tag{36}$$

Note that the "gauge" piece $q_\mu q_\nu/m_\rho^2$ will not contribute to the RPA response because in the mean-field approximation the vector-isovector current is conserved. For the $NN\pi$ vertex we have adopted a pseudovector form with $f_\pi^2/4\pi = 0.075$. The pion, rho, and free nucleon masses have been fixed at their experimental values.

The most uncertain parameter in our calculation is the phenomenological Landau-Migdal parameter g'. Traditionally, g' is introduced to regularize the large spin-spin component of the isovector interaction. In a relativistic formalism we can incorporate short-range correlation effects by modifying the pion "propagator" in the following way:

$$V_{\mu\nu} = \frac{q_\mu q_\nu}{q^2 - m_\pi^2 + i\epsilon} \rightarrow V_{\mu\nu} = \frac{q_\mu q_\nu}{q^2 - m_\pi^2 + i\epsilon} - g' g_{\mu\nu} \ . \tag{37}$$

Without g' the contribution of the pion to the RPA response would be suppressed by current conservation and the small leptonic mass. Therefore, it is through the Landau-Migdal parameter g' that the pion mainly contributes to the RPA response (note that the term proportional to g' has, both, longitudinal as well as transverse components). With this choice for the pion propagator the "elementary" $NN\pi$ vertex becomes

$$\Gamma_{NN\pi}^\mu = \sqrt{2}\frac{f_\pi}{m_\pi}\gamma^5\gamma^\mu \ . \tag{38}$$

With the above Feynman rules in hand we can now construct the medium-modified rho- and pion-mediated interactions. Note that the inclusion of g', which contains transverse as well as longitudinal components, is responsible for ρ-π mixing. In order to account properly for this mixing, Dyson's equation for the propagator must be expanded from a 4×4 to an 8×8 matrix equation:

$$\mathbf{D}_{\rm RPA} = \mathbf{D}_0 + \mathbf{D}_0\boldsymbol{\Pi}_0\mathbf{D}_{\rm RPA} \ , \tag{39}$$

where we have defined the free (diagonal) propagator matrix

$$\mathbf{D}_0 = \begin{pmatrix} \mathbf{R} & \mathbf{0} \\ \mathbf{0} & \mathbf{V} \end{pmatrix} , \tag{40}$$

in terms of the ρ- [Eq. (36)] and g'-modified pion propagator [Eq. (37)]. We have also introduced the mixed ρ-π polarization matrix

$$\boldsymbol{\Pi}_0 = \begin{pmatrix} \boldsymbol{\Pi}_{\rho\rho} & \boldsymbol{\Pi}_{\rho\pi} \\ \boldsymbol{\Pi}_{\pi\rho} & \boldsymbol{\Pi}_{\pi\pi} \end{pmatrix} , \tag{41}$$

with individual components given by

$$\Pi_{\rho\rho}^{\mu\nu} = -\frac{i}{2}\int\frac{d^4p}{(2\pi)^4}\,{\rm Tr}\left[\left(g_\rho\gamma^\mu + \frac{if_\rho\sigma^{\mu\alpha}q_\alpha}{2M}\right)G(p)\left(g_\rho\gamma^\nu - \frac{if_\rho\sigma^{\nu\beta}q_\beta}{2M}\right)G(p+q)\right] , \tag{42}$$

$$\Pi_{\rho\pi}^{\mu\nu} = \Pi_{\pi\rho}^{\mu\nu} = -\frac{ig_\rho f_\pi}{m_\pi}\int\frac{d^4p}{(2\pi)^4}\,{\rm Tr}\left[\left(\gamma^\mu + \frac{if_\rho\sigma^{\mu\alpha}q_\alpha}{2Mg_\rho}\right)G(p)\gamma^5\gamma^\nu G(p+q)\right] , \tag{43}$$

$$\Pi_{\pi\pi}^{\mu\nu} = -\frac{i2f_\pi^2}{m_\pi^2}\int\frac{d^4p}{(2\pi)^4}\,{\rm Tr}[\gamma^5\gamma^\mu G(p)\gamma^5\gamma^\nu G(p+q)] \ . \tag{44}$$

The RPA correction to the polarization now takes the following form [see Fig. 2(a)]:

$$\boldsymbol{\Delta\Pi}_{\rm RPA} = (\boldsymbol{\Pi}_\rho, \boldsymbol{\Pi}_\pi)\,\mathbf{D}_{\rm RPA}\begin{pmatrix} \boldsymbol{\Pi}_\rho \\ \boldsymbol{\Pi}_\pi \end{pmatrix} , \tag{45}$$

where $\boldsymbol{\Pi}_\rho$ and $\boldsymbol{\Pi}_\pi$ characterize the in-medium mixing — due to particle-hole excitations — of a charged weak-vector boson with a ρ or π meson, respectively, and are given by

$$\Pi_\rho^{\mu\nu} = -i\frac{g_\rho}{\sqrt{2}}\int\frac{d^4p}{(2\pi)^4}\,{\rm Tr}\left[\Gamma^\mu G(p)\left(\gamma^\nu - \frac{if_\rho\sigma^{\nu\alpha}q_\alpha}{2Mg_\rho}\right)G(p+q)\right] , \tag{46}$$

$$\Pi_\pi^{\mu\nu} = -\sqrt{2}i\frac{f_\pi}{m_\pi}\int\frac{d^4p}{(2\pi)^4}\,{\rm Tr}[\Gamma^\mu G(p)\gamma^5\gamma^\nu G(p+q)] \ . \tag{47}$$

An RPA calculation of the inclusive response uses the same expression for the cross section as in Eq. (12) with the replacement:

$$\Pi^{\mu\nu} \rightarrow \Pi^{\mu\nu}_{\rm RPA} = \Pi^{\mu\nu} + \Delta\Pi^{\mu\nu}_{\rm RPA} \ . \tag{48}$$

In an impulse (or uncorrelated) description of the response the cross section is only sensitive to the imaginary part of the lowest-order polarizations. Since the nuclear response is being probed in the spacelike ($q^2 < 0$) region, $N\bar{N}$ pairs cannot be excited in these lowest-order descriptions. They can, however, be virtually excited and, thus, will become an essential ingredient of the RPA response. Traditionally, $N\bar{N}$ excitations have been divided into two contributions, one being vacuum polarization and the other consisting of the Pauli blocking of $N\bar{N}$ excitations due to the filled Fermi sea [14]. The latter contribution is finite and has been shown to be essential for the conservation of the electromagnetic current. This contribution has been included in our calculations. The former, however, is divergent and must be renormalized. Since we are using a nonrenormalizable theory with derivative couplings, the renormalization of these divergent contributions becomes ambiguous at best. Thus, in order to avoid including *ad hoc* parameters (e.g., cutoffs) we have decided to simply ignore the effect from vacuum polarization. Note that the (finite) real parts of the various polarizations have been calculated analytically and most of them have been published already [20]. Here we calculate them numerically so we can extend the formalism to include momentum-dependent self-energies.

D. Momentum-dependent vector and scalar self-energy

In a mean-field approximation to the Walecka model the vector (V) and scalar (S) self-energies are replaced by their classical expectation values. In this approximation the nucleon self-energy is real and energy independent. However, as the momentum of the nucleon becomes large there is an important coupling of the nucleon to nuclear excitations. Indeed, at intermediate energies it is known that the reactive content of the reaction is dominated by quasifree nucleon knockout. Thus, at large enough momentum the nucleon self-energy will become complex and energy dependent. In order to calculate the nuclear response for a broad range of momentum transfers, we incorporate momentum-dependent self-energies into the nucleon propagator. Since a microscopic calculation of the energy dependence of the nucleon self-energy in the Walecka model awaits, we have used the phenomenological optical potentials of Ref. [21]. A detailed discussion of this momentum-dependent correction can be found in Ref. [22].

In a calculation with momentum-dependent self-energies, the effective mass and energy of nucleons in the medium are no longer constant. In particular, the nucleon propagator must now be described in terms of Dirac spinors with masses and energies given by

$$M^*_{\mathbf{p}} = M + S(\mathbf{p}) \ ,$$
$$E_{\mathbf{p}} = E^*_{\mathbf{p}} + V(\mathbf{p}) = \sqrt{\mathbf{p^2} + M^{*2}_{\mathbf{p}}} + V(\mathbf{p}) \ . \tag{49}$$

The basic formalism, however, remains unchanged except for the inclusion of a more realistic nucleon propagator given by

$$G(p) = (\not{p}^* + M^*_{\mathbf{p}}) \Bigg[\frac{1}{p^{*2} - M^{*2}_{\mathbf{p}} + i\epsilon} + \frac{i\pi}{E^*_{\mathbf{p}}} \delta(p^*_0 - E^*_{\mathbf{p}}) \theta(k_F - |\mathbf{p}|) \Bigg] \ , \tag{50}$$

where $p^{*\mu} = [p^0 - V(\mathbf{p}), \mathbf{p}]$. Note that the vector potential can no longer be eliminated from the integrals defining the polarization by a simple change of variables.

III. RESULTS

In this section we present results for the inclusive cross section using a variety of approximations. We consider impulse-approximation calculations using, both, a relativistic Fermi gas of nucleons of mass M and a self-consistent ground state with an effective nucleon mass of M^*. We also present two calculations including RPA correlations either with mass M or M^*. The mass M RPA calculations can be directly compared to similar nonrelativistic calculations. Finally, results will be shown using momentum-dependent self-energies obtained from the phenomenological fit to the nucleon optical potential of Ref. [21]. We refer to this last calculation as impulse with $M^*_{\mathbf{p}}$. The impulse with M calculation is commonly used to extract from experiment the mass parameter M_A present in the dipole fit to the axial form factor G_A. Our main goal is to estimate the sensitivity of this parameter to various relativistic nuclear-structure effects.

The effective nucleon mass M^* (in mean-field theory) is obtained from a solution to the self-consistency equation [11],

$$M^* = M - \frac{g_s^2}{m_s^2} \frac{4}{(2\pi)^3} \int_0^{k_F} d^3k \frac{M^*}{\sqrt{\mathbf{k}^2 + M^{*2}}} \ . \tag{51}$$

Choosing the couplings to reproduce the bulk properties of nuclear matter at saturation [$g_s^2(M^2/m_s^2) = 267.1$] leads to a value of the effective nucleon mass of $M^* = 638$ MeV at an assumed average density corresponding to $k_F = 225$ MeV.

In Fig. 3 we show the double differential cross section $d^2\sigma/d\Omega_{k'}dE_\mu$ [see Eq. (12)] for a neutrino energy of $E_\nu = 1$ GeV. Figure 3(a) is for a momentum transfer of $|\mathbf{q}| = 0.5$ GeV while Fig. 3(b) is for $|\mathbf{q}| = 1.2$ GeV. At $|\mathbf{q}| = 0.5$ GeV the peak positions from the M^* and $M^*_{\mathbf{p}}$ calculations are shifted by less than 50 MeV relative to the Fermi-gas peak. This value represents an average binding-energy shift and has been observed experimentally in quasielastic electron scattering. Thus, a simple mean-field calculation is expected to give a reasonable description of the nuclear response. The situation changes considerably, however, at $|\mathbf{q}| = 1.2$ GeV [Fig. 3(b)]. Here, the M^* calculation predicts a shift in the peak position

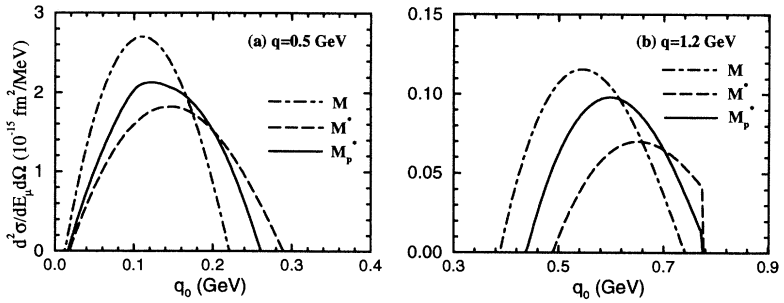

FIG. 3. Double differential cross sections for 1 GeV neutrinos. The solid curve is the momentum-dependent calculation. (a) is for $|\mathbf{q}| = 0.5$ GeV while (b) is for $|\mathbf{q}| = 1.2$ GeV. The dashed (dot-dashed) curve is the cross section obtained from a MFT (free Fermi gas) calculation.

that is substantially larger than the one obtained using the more realistic ($M^*_{\mathbf{p}}$) self-energies. Note that the impulse with $M^*_{\mathbf{p}}$ calculation still predicts a substantial shift (of the order of 50 MeV) relative to the Fermi-gas value. Also note the kinematical cutoff in q_0 — above this value the scattering is prohibited kinematically. The impulse with M^* calculation has a considerable amount of strength shifted into this inaccessible region. At this momentum transfer, the mean-field calculation overpredicts the binding energy shift seen in electron scattering [22,23]. In contrast, the calculation using the impulse with $M^*_{\mathbf{p}}$ shows a reasonable binding-energy shift and is practically insensitive to the kinematical cutoff.

Figure 4 shows the inclusive RPA cross section at $|\mathbf{q}| = 0.5$ GeV for various values of the Landau-Migdal parameter g'. For reference, the impulse results with M and with M^* have also been included in Fig. 4(c). The solid line shows the RPA response of a Fermi gas ground state while the dashed line shows the RPA response of the mean-field ground state. Since the pion contributes only through g', the softening and enhancement of the response in Fig. 4(a) is exclusively due to an attractive, and thus unrealistic, rho-mediated residual interaction.

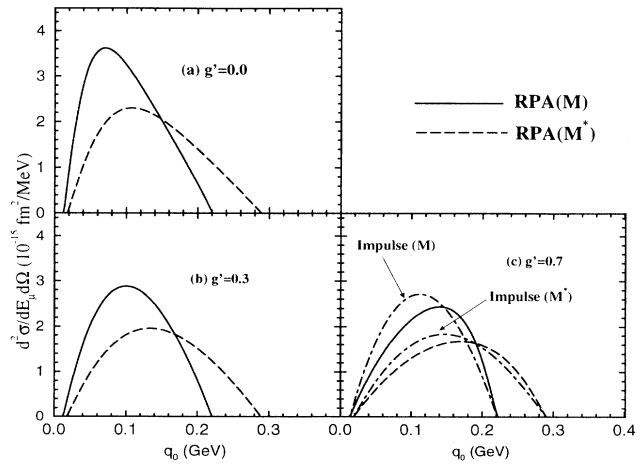

FIG. 4. Double differential cross section with RPA correlations for $|\mathbf{q}| = 500$ MeV and $E_\nu = 1$ GeV. The solid curve is the RPA calculation with M while the dashed curve is the RPA with M^*. (a) is for g'=0, (b) is for g'=0.3, and (c) is for g'=0.7. In (c) the M and M^* impulse calculations are also shown for comparison.

As the value of g' is increased to $g' = 0.3$, the peak moves to higher excitation energy, and the overall strength of the response is reduced. This is consistent with an additional repulsive component to the residual interaction arising from g'. Finally, Fig. 4(c) shows the RPA results using the standard value of $g' = 0.7$. One now observes a slight quenching and hardening of the response due to the large value of g'.

Since most of the experiments report the energy-integrated cross section $d\sigma/dQ^2$ we have taken our results for the double differential cross section and integrated over the allowed kinematical region of q_0

$$\frac{d\sigma}{dQ^2} = \int_0^{Q_c} \frac{\pi}{E_\nu k'} \frac{d^2\sigma}{dE_\mu d\Omega} dq_0 \ , \tag{52}$$

where the energy cutoff is given by

$$Q_c = E_\nu + \frac{q^2 - m_\mu^2}{4E_\nu} + \frac{E_\nu m_\mu^2}{q^2 - m_\mu^2} \ , \tag{53}$$

and m_μ is the mass of the produced lepton. In Fig. 5(a) the energy-integrated cross section, $d\sigma/dQ^2$, at $E_\nu = 1.2$ GeV is shown for three calculations: impulse with M, RPA with M^* using $g' = 0.7$, and impulse with $M^*_{\mathbf{p}}$. Note that there is a substantial quenching due to RPA correlations at small momentum transfers, i.e., $Q^2 \leq 0.3$ GeV^2. In the intermediate range ($0.3 \leq Q^2 \leq 0.9$ GeV^2) the importance of RPA correlations diminishes, and no signifi-

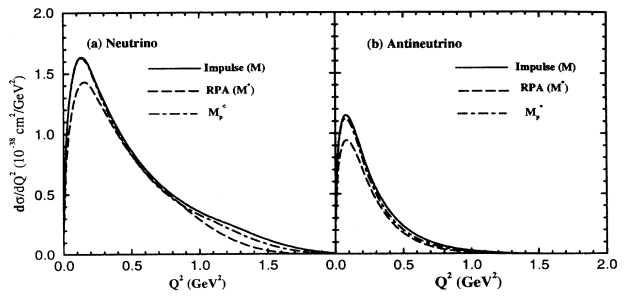

FIG. 5. $d\sigma/dQ^2$ for a neutrino (a) and antineutrino (b) scattering at an incoming energy of 1.2 GeV. The solid curve is the impulse with M calculation while the dashed curve is the M^* RPA with $g' = 0.7$. The effect of the momentum-dependent self-energies is indicated with the dot-dashed line.

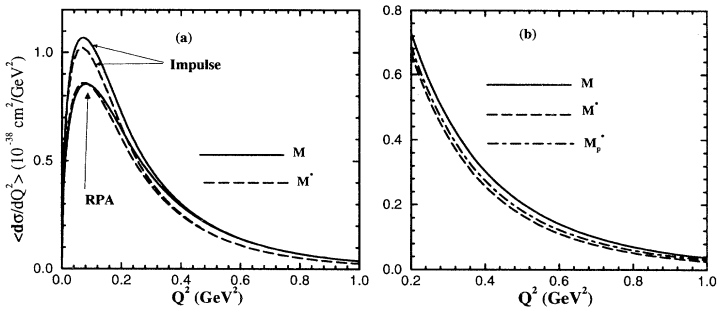

FIG. 6. $d\sigma/dQ^2$ averaged over the BNL spectrum. In (a) the two solid curves denote the impulse and the RPA ($g' = 0.7$) results using the free nucleon mass M. Also shown (two dashed lines) are the corresponding results using an effective nucleon mass M^*. In (b) the cross sections are shown over the available experimental range in Q^2. The solid and the dashed curves are the results of impulse calculations with M and M^*, respectively. The dot-dashed curve is the calculation with momentum-dependent self-energies.

cant differences are observed between the three models. At an even larger Q^2 the RPA curve splits from the other two indicating the breakdown of the mean-field approximation [see Fig. 3(b)]. This breakdown, however, is not associated to RPA effects, which are no longer effective at this momentum transfer, but rather from the mean-field M^* effects. Indeed, an RPA calculation using the free nucleon mass is within one percent of the impulse with M calculation at high Q^2.

We report similar calculations for antineutrinos in Fig. 5(b). The cross sections are considerably reduced relative to neutrinos because of the sign change in the vector-axial interference term [see Eq. (23)]. In addition, since the cross sections fall to (almost) zero for $Q^2 \geq 1$ GeV^2, most of the quasifree strength is located below the cutoff Q_c. Hence, the kinematical cutoff does not have a significant effect on the M^* curve at large Q^2. At a smaller momentum transfer, $Q^2 \leq 0.3$ GeV^2, and just as in the neutrino case, RPA correlations substantially reduce the cross section. At a larger Q^2, most of the differences observed between the RPA and the impulse with M calculations are due to the strong scalar potential. The impulse with M^*_{p} calculation (dot-dashed curve) smoothly interpolates these two models.

In the BNL experiment [8], the axial mass M_A, which controls the Q^2 falloff of the axial form factor [see Eq. (A9)], was extracted from antineutrino data using a Fermi gas (i.e., impulse with M) formalism. From an analysis of their data in the range $Q^2 = 0.2$–1 GeV^2, the BNL group extracted a value of $M_A = 1.09 \pm 0.03$ (stat) ± 0.02 (syst) GeV. In Fig. 6 we show the cross section, $d\sigma/dQ^2$, averaged over the BNL neutrino spectrum. In Fig. 6(a) we present four different calculations: impulse and RPA with M (solid lines), and impulse and RPA with M^* (dashed lines). The two curves using the free nucleon mass M start to overlap at $Q^2 = 0.4$ GeV^2 and, insofar as we can regard them as our nonrelativistic limit, they agree with the nonrelativistic results obtained by Singh and Oset [9]. Similarly, the two M^* curves also coincide for $Q^2 \geq 0.4$ GeV^2 illustrating the fact that RPA correlations become unimportant in this Q^2 region. In Fig. 6(b) we show three impulse curves in the $Q^2 = 0.2$–1 GeV^2 range — the region sampled in the BNL experiment. At $Q^2 = 0.2$ there is a six percent difference between the impulse with M calculation and the M^* and M^*_{p} values. This difference becomes larger, 20–30 %, at $Q^2 = 1.0$ GeV^2. It is, therefore, essential to estimate the sensitivity of M_A to these nuclear-structure effects.

The raw experimental data as a function of the four-momentum transfer Q^2 was fitted with a theoretical curve to determine M_A. Since the experiment suffers from an uncertainty in the overall normalization, we use the ratio of the cross section at two different values of Q^2 to extract M_A. In Table I we show the ratio of the cross section using $Q^2 = 0.2$ GeV^2 and $Q^2 = 1.0$ GeV^2. The value of the axial-mass parameter M_A was varied in the $1.09 - 1.30$ GeV range, and the ratio of cross sections reported for various nuclear-structure models. For $M_A = 1.09$ GeV, the value extracted from the BNL data, the impulse with M ratio equals 19.42. This represents our baseline value for the ratio. In order to reproduce this value using the impulse with M^* calculation the value of the axial-mass must be changed to $M_A = 1.30$ GeV (a 20% increase). Similarly, the value of M_A must be changed to 1.25 GeV in the RPA with M^* and to 1.20 GeV in the M^*_{p} calculation. There is, however, no M_A

TABLE I. The ratio of cross section $\frac{d\sigma}{dQ^2}(Q^2 = 0.2\,\mathrm{GeV}^2)/\frac{d\sigma}{dQ^2}(Q^2 = 1.0\,\mathrm{GeV}^2)$ for various nuclear structure effects at a given axial mass M_A in the first column.

	$\frac{d\sigma}{dQ^2}(Q^2 = 0.2\,\mathrm{GeV}^2)/\frac{d\sigma}{dQ^2}(Q^2 = 1.0\,\mathrm{GeV}^2)$				
M_A (GeV)	Impulse M	Impulse M^*	RPA M^*	RPA M	M^*_{p}
1.09	19.42	25.83	23.72	17.21	21.85
1.14	18.47	24.71	22.59	16.32	20.83
1.18	17.75	23.78	21.69	15.66	20.03
1.21	16.91	22.66	20.61	14.89	19.08
1.25	15.95	21.36	19.38	14.02	18.00
1.30	14.9	19.92	18.04	13.07	16.81

TABLE II. The same as Table I for the ratios $\frac{d\sigma}{dQ^2}(Q^2 = 0.5\,\mathrm{GeV}^2)/\frac{d\sigma}{dQ^2}(Q^2 = 1.0\,\mathrm{GeV}^2)$.

	$\frac{d\sigma}{dQ^2}(Q^2 = 0.5\,\mathrm{GeV}^2)/\frac{d\sigma}{dQ^2}(Q^2 = 1.0\,\mathrm{GeV}^2)$				
M_A (GeV)	Impulse M	Impulse M^*	RPA M^*	RPA M	$M_{\mathbf{p}}^*$
1.09	5.47	6.50	6.40	5.34	5.77
1.14	5.35	6.38	6.27	5.21	5.65
1.18	5.24	6.26	6.14	5.10	5.54
1.21	5.10	6.09	5.96	4.96	5.39
1.25	4.92	5.88	5.75	4.78	5.21
1.30	4.72	5.62	5.49	4.58	4.99

value within this range that can reproduce the ratio using an RPA with M calculation. This is because RPA effects substantially reduce the cross section at $Q^2 = 0.2$ (about 10%) which was not expected from nonrelativistic calculations.

Since we have established that RPA correlations become unimportant for $Q^2 \geq 0.4$ GeV^2, we can eliminate the sensitivity to RPA effects by computing the ratio of cross sections using $Q^2 = 0.5$ GeV^2 and $Q^2 = 1.0$ GeV^2 (see Table II). In this case, using the impulse with M calculation we obtain a baseline value for the ratio of 5.47 at $M_A = 1.09$ GeV. Now the RPA with M does not induce any change in the value of M_A — in agreement with the nonrelativistic calculation of Singh and Oset [9]. This, however, is not the case for the other nuclear-structure calculations. Indeed, even in the impulse with $M_{\mathbf{p}}^*$ calculation, which generates the smallest change, a 10% increase in the value of M_A is required. This 10% uncertainty in the value of M_A could complicate the extraction of strange-quark matrix elements from experimental studies of neutral weak form factors [7]. Note that since the $M_A = 1.09$ GeV number is already larger than the world-average value of $M_A = (1.032 \pm 0.036)$ GeV, nuclear-structure corrections make the discrepancy even larger.

IV. CONCLUSIONS AND OUTLOOK

We have used a relativistic formalism to study inclusive charged-current neutrino scattering in an impulse approximation. The nuclear-structure information is contained in a large set of nuclear-response functions that were evaluated in nuclear matter using a variety of approximations. The simplest approximation that we considered was a relativistic free Fermi gas. This approximation was used by the BNL group to extract the axial mass parameter M_A. We have used the Fermi-gas approximation, together with the BNL-extracted value of $M_A = 1.09$ GeV, to fix the Q^2 dependence of the inclusive cross section. We have examined the sensitivity of this extracted value for M_A to various nuclear-structure effects, such as the ones arising from the mean fields (M^*), RPA correlations, and momentum-dependent self-energies. In essence, we have computed the changes in M_A that were required to reproduce the baseline free Fermi-gas cross section once these additional nuclear-structure effects were taken into consideration. This analysis is useful because a robust value of M_A is essential for a reliable determination of the strange-quark content of the nucleon.

Our results indicate important corrections to the nuclear response due to the mean fields (M^*) and to RPA correlations. Indeed, changes as large as 20% in M_A were observed whenever the whole range of Q^2 values (0.2 GeV$^2 \leq Q^2 \leq 1.0$ GeV^2) used in the BNL experiment were employed for the extraction. This uncertainty, however, can be substantially reduced. For example, it is well known that RPA correlations are effective only at small-momentum transfers (i.e., $Q^2 \leq 0.3$ GeV^2). In addition, phenomenological fits to the nucleon optical potential indicate that, at large nucleon momenta, the mean fields are considerably smaller in magnitude than the ones predicted by the mean-field theory. Hence, some of the nuclear-structure uncertainties can be removed by employing phenomenological (momentum-dependent) mean fields and by restricting the range of Q^2 to the region 0.5 GeV$^2 \leq Q^2 \leq 1.0$ GeV^2. Note that, although weaker than in the mean-field theory, the momentum-dependent optical potentials are still large and induce nontrivial changes in the effective mass and energy of a particle in the medium. Indeed, even in this best-case scenario a 10% uncertainty in M_A persists. With this extra 10% uncertainty, the BNL experiment [4] by itself no longer provides strong evidence for a nonzero strangeness content of the nucleon [7].

Garvey and collaborators [24] have proposed to extract the strange axial-vector form factor from a measurement of the ratio of neutron to proton yields in neutrino-induced reactions. Taking the ratio will cancel some of the (isoscalar) nuclear-structure uncertainties. However, the low-energy quasielastic (ν_μ, μ^-) cross section was recently measured to be less than half of that of a free Fermi gas [25]. This indicates that nuclear-structure effects might be very large [26] at the low energies sampled in the LSND experiment. Therefore, it is important to investigate nuclear-structure effects, such as RPA correlations, in the neutron to proton ratio.

In the future we will employ the present relativistic RPA formalism to calculate the inclusive cross section for atmospheric neutrinos. Atmospheric neutrinos have been observed over a wide range of energies (from a few hundred MeV to several GeV) in large water Čerenkov detectors — hence the need for a formalism that can address neutrino physics over this broad energy range. Atmospheric neutrinos are particularly interesting because of the current flavor anomaly in the ν_μ/ν_e ratio. This anomaly might signal neutrino oscillations. However, first one must rule out all conventional nuclear effects. Thus, it is important to examine these nuclear-structure corrections before a definitive statement about new physics can be made.

ACKNOWLEDGMENTS

We would like to thank David K. Griegel for careful reading of the manuscript and valuable comments. We also thank Stefan Schramm for various suggestions. This

research was supported by the U.S. Department of Energy under Grant No. DE-FG02-87ER-40365, DE-FC05-85ER250000, and DE-FG05-92ER40750.

APPENDIX A

We adopt the form factor parametrization used in Ref. [5]. First, the electromagnetic form factors are written in terms of simple dipole forms:

$$G = (1 + 4.97\tau)^{-2},\ \tau = -q^2/4M^2, \tag{A1}$$

$$F_1^{(p)} = [1 + \tau(1 + \lambda_p)]G/(1 + \tau), \tag{A2}$$

$$F_2^{(p)} = \lambda_p G/(1 + \tau), \tag{A3}$$

$$F_1^{(n)} = \tau\lambda_n(1 - \eta)G/(1 + \tau), \tag{A4}$$

$$F_2^{(n)} = \lambda_n(1 + \tau\eta)G/(1 + \tau). \tag{A5}$$

Here the anomalous moments are

$$\lambda_p = 1.793,\quad \lambda_n = -1.913, \tag{A6}$$

and

$$\eta = (1 + 5.6\tau)^{-1}. \tag{A7}$$

This parametrization is good for the neutron form factors provided $\tau \ll 1$. The isovector form factors are given by

$$F_1 = F_1^{(p)} - F_1^{(n)},\quad F_2 = F_2^{(p)} - F_2^{(n)}. \tag{A8}$$

The axial form factor G_A is

$$G_A = \frac{1.26}{(1 - q^2/M_A^2)^2}, \tag{A9}$$

and the pseudoscalar form factor is given by

$$F_p = \frac{2MG_A}{m_\pi^2 - q^2}. \tag{A10}$$

APPENDIX B

Analytic expressions for the imaginary parts of the polarizations introduced in Sec. II B are

$$\mathrm{Im}(\Pi_L^{vv}) = \frac{q^2}{2\pi\mathbf{q}^3}\left[E_3 + q_0E_2 + \frac{q^2E_1}{4}\right], \tag{B1}$$

$$\mathrm{Im}(\Pi_T^{vv}) = \frac{q^2}{4\pi\mathbf{q}^3}\left[E_3 + q_0E_2 + \left(\frac{\mathbf{q}^2M^{*2}}{q^2} + \frac{q_0^2 + \mathbf{q}^2}{4}\right)E_1\right], \tag{B2}$$

$$\mathrm{Im}(\Pi_L^{tt}) = \frac{-q^2}{8\pi\mathbf{q}^3M^2}\left[q^2E_3 + q_0q^2E_2 + \left(M^{*2}\mathbf{q}^2 + \frac{q^2q_0^2}{4}\right)E_1\right], \tag{B3}$$

$$\mathrm{Im}(\Pi_T^{tt}) = \frac{q^2}{16\pi\mathbf{q}^3M^2}\left[\left(M^{*2}\mathbf{q}^2 - \frac{q^4}{4}\right)E_1 - q_0q^2E_2 - q^2E_3\right], \tag{B4}$$

$$\mathrm{Im}(\Pi_A) = \frac{M^{*2}E_1}{2\pi|\mathbf{q}|}, \tag{B5}$$

$$\mathrm{Im}(\Pi_L^{vt}) = \frac{-q^2M^*E_1}{8\pi|\mathbf{q}|M} = -\mathrm{Im}(\Pi_T^{vt}), \tag{B6}$$

$$\mathrm{Im}(\Pi_{va}) = \frac{q^2}{8\pi\mathbf{q}^3}[2E_2 + q_0E_1], \tag{B7}$$

$$\mathrm{Im}(\Pi_{pp}) = \frac{q^2E_1}{8\pi|\mathbf{q}|}, \tag{B8}$$

$$\mathrm{Im}(\Pi_{ap}) = -\frac{M^*E_1}{4\pi|\mathbf{q}|}, \tag{B9}$$

where

$$E_n = \frac{E_F^n - E_-^n}{n},\quad (n = 1, 2, 3), \tag{B10}$$

with

$$E_F = \sqrt{k_F^2 + M^{*2}}, \tag{B11}$$

$$E_- = \min(E_F, E_{\max}), \tag{B12}$$

$$E_{\max} = \max\left[M^*, E_F - q_0, \frac{1}{2}\left(-q_0 + |\mathbf{q}|\sqrt{1 - \frac{4M^{*2}}{q^2}}\right)\right]. \tag{B13}$$

The vacuum part does not contribute to the impulse response for spacelike momenta.

[1] J. Ashman *et al.*, Phys. Lett. B **206**, 364 (1988); Nucl. Phys. **B328**, 1 (1989).
[2] M.J. Musolf and Barry R. Holstein, Phys. Lett. B **242**, 461 (1990).
[3] R.D. McKeown, Phys. Lett. B **219**, 140 (1989).
[4] L.A. Ahrens *et al.*, Phys. Rev. D **35**, 785 (1987).
[5] M.J. Musolf and T.W. Donnelly, Nucl. Phys. **A546**, 509 (1992).
[6] G.T. Garvey, W.C. Louis, and D.H. White, Phys. Rev. C **48**, 761 (1993).
[7] C.J. Horowitz, Hungchong Kim, D. Murdock, and S. Pollock, Phys. Rev. C **48**, 3078 (1993).
[8] L.A. Ahrens *et al.*, Phys. Lett. B **202**, 284 (1988).
[9] S.K. Singh and E. Oset, Nucl. Phys. **A542**, 587 (1992).

[10] S. Bonnetti *et al.*, Nuovo Cimento A **38**, 260 (1977); M. Pohl *et al.*, Lett. Nuovo Cimento **26**, 332 (1979); N. Armenis *et al.*, Nucl. Phys. **B152**, 365 (1979).
[11] B.D. Serot and J.D. Walecka, in *Advances in Nuclear Physics*, edited by J.W. Negele and E. Vogt (Plenum, New York, 1986), Vol. 16.
[12] C.J. Horowitz and J. Piekarewicz, Phys. Rev. C **47**, 2924 (1993).
[13] A.L. Fetter and J.D. Walecka, *Quantum Theory of Many-Particle Systems* (McGraw-Hill, New York, 1971).
[14] C.J. Horowitz and J. Piekarewicz, Nucl. Phys. **A511**, 461 (1990).
[15] John F. Dawson and R.J. Furnstahl, Phys. Rev. C **42**, 2009 (1990).
[16] C.J. Horowitz, Nucl. Phys. **A412**, 228 (1984).
[17] C.J. Horowitz and J. Piekarewicz, Phys. Lett. B **301**, 321 (1993); Phys. Rev. C **50**, 2540 (1994).
[18] J. Engel, E. Kolbe, K. Langanke, and P. Vogel, Phys. Rev. D **48**, 3048 (1993).
[19] R. Machleidt, K. Holinde, and Ch. Elster, Phys. Rep. **149**, 1 (1987).
[20] K. Lim and C.J. Horowitz, Nucl. Phys. **A501**, 729 (1989); Haruki Kurasawa and Toshio Suzuki, *ibid.* **A445**, 685 (1985).
[21] E.D. Cooper, S. Hama, B.C. Clark, and R.L. Mercer, Phys. Rev. C **47**, 297 (1993).
[22] Hungchong Kim, C.J. Horowitz, and M.R. Frank, Phys. Rev. C **51**, 792 (1995).
[23] M.R. Frank, Phys. Rev. C **49**, 555 (1994).
[24] G.T. Garvey, E. Kolbe, K. Langanke, and S. Krewald, Phys. Rev. C **48**, 1919 (1993).
[25] M. Albert *et al.*, LANL Bulletin Board Report No. nucl-th-9410039.
[26] J. Piekarewicz, Hungchong Kim, and C. J. Horowitz, Phys. Lett. B (submitted).